ASYMPTOTIC METHODS FOR INTERNAL TRANSONIC FLOWS

T.C. Adamson, Jr.
A.F. Messiter
The University of Michigan
Ann Arbor, Michigan

SUMMARY

For many internal transonic flows of practical interest, some of the relevant nondimensional parameters typically are small enough that a perturbation scheme can be expected to give a useful level of numerical accuracy. A variety of steady and unsteady transonic channel and cascade flows is studied with the help of systematic perturbation methods which take advantage of this fact. Asymptotic representations are constructed for small changes in channel cross-section area, small flow deflection angles, small differences between the flow velocity and the sound speed, small amplitudes of imposed oscillations, and small reduced frequencies. Inside a channel the flow is nearly one-dimensional except in thin regions immediately downstream of a shock wave, at the channel entrance and exit, and near the channel throat. A study of two-dimensional cascade flow is extended to include a description of three-dimensional compressor-rotor flow which leads to analytical results except in thin edge regions which require numerical solution. For unsteady flow the qualitative nature of the shock-wave motion in a channel depends strongly on the orders of magnitude of the frequency and amplitude of impressed wall oscillations or fluctuations in back pressure. One example of supersonic flow is considered, for a channel with length large compared to its width, including the effect of separation bubbles and the possibility of self-sustained oscillations. The effect of viscosity on a weak shock wave in a channel is discussed.

1. INTRODUCTION

Systematic asymptotic methods of analysis have been in use for roughly thirty years, in a wide variety of perturbation problems. Although they have proven to be quite useful in general, there are several classes of problems in fluid mechanics in which they are particularly powerful, not only because they provide relatively simple formulations for quite complex flows, but also because they emphasize and illuminate regions of particular physical and mathematical importance. This has been true in flow problems involving viscous-inviscid interactions, for example, and in the subject area of this paper, internal inviscid transonic flows (refs. 1-33).

There are several reasons for the success of asymptotic methods in internal transonic flows. One is that small changes in cross-sectional area cause relatively large changes in flow velocity, and so perturbation methods are particularly appropriate. Most important, however, is the well-known fact that the nonlinear small-disturbance equation, which generally holds in some part of a transonic flow field, is valid in regions for which the characteristic length in the flow direction is small compared to that in the lateral direction. Thus, in transonic flow over an isolated airfoil, lengths in the flow direction are scaled by the chord but the proper scale in the transverse direction is large in comparison with the chord. In internal flows, however, the lengths in the transverse direction are constrained by the channel walls. Hence, regions where the nonlinear equation may be required are small in the flow direction, i.e. they are "inner" regions; by far the major part of the flow field is governed by simpler equations, one-dimensional to lowest order. It will be seen that inner solutions are needed at the throat of a channel, immediately downstream of a shock wave, at the entrance and exit of a diffuser, and at the leading and trailing edges of cascades. Still further simplifications follow in certain important limiting cases for which the inner regions (except perhaps at the throat) are described by linearized two-dimensional equations. Finally, it may be noted that in transonic channel flows with shock waves,

PRECEDING PAGE BLANK NOT FILMED

only small changes in downstream pressure or wall shape are sufficient to give large changes in position of the shock wave. Hence , the fact that perturbation theory is employed does not restrict the physical problem to one in which only small changes in every variable are allowed. Problems of significant technical interest can be considered using asymptotic techniques.

Of the early attempts to obtain solutions for transonic channel flows, two groups of studies have special bearing on the subject of this paper, the use of systematic asymptotic methods of formulation. The first of these covers work initiated in a paper by Tomotika and Tamada (ref. 1), in which similarity solutions to the nonlinear small-disturbance equation are introduced. As is usual with similarity solutions, it is not possible to select arbitrary wall shapes at which boundary conditions may be imposed; instead one accepts the solution as given and chooses one of the streamlines as a wall. However, the solutions given by Tomotika and Tamada were very informative in illustrating the way in which a flow accelerates from subsonic through sonic to supersonic conditions (Meyer flow) and the way in which supersonic pockets form along the walls and grow as the pressure ratio across the channel increases (Taylor flow). It was found by Sichel (ref. 2), in his study of nozzle flows, and also by Ryzhov (ref. 3), that this similarity transformation can be used when the longitudinal viscosity is such that a shock wave of non-negligible thickness is formed. Indeed, the transformation holds for nozzle flows in which the shock wave is infinitesimally thin as well (ref. 4). Because the flow is deflected slightly as it passes through a nearly normal shock wave, the streamlines through a thin shock have a kink at the wave and through a thick shock are bent while passing through the wave. Hence, the interpretation of a streamline as being equivalent to a wall is not obvious, especially if a channel with varying back pressure and thus varying shock-wave positions is being considered. In these studies no order estimates of characteristic lengths are given and, indeed, there was some controversy among workers in the field about the extent of the flow field over which these solutions held.

It was found that the similarity transformation of Tomotika and Tamada could be extended to unsteady flows with a relatively simple modification (ref. 5), and this fact was exploited to cover unsteady flows with either thick or thin shock waves (ref. 4). In the latter reference, an inner region in which the structure of the shock wave was calculated was employed for the case where the shock was thin. In all other aspects, the solutions are similarity solutions so that streamlines move with time and at the shock wave again have a bend which now moves with the wave. Nevertheless, unsteady Meyer and Taylor flows are shown as is the structure of moving shock waves, all with very little computational effort; thus, such solutions are very informative but not particularly useful insofar as use in channel design is concerned.

The second group of papers which are particularly relevant begins with a paper by Szaniawski (ref. 6), in which he introduced a power-series solution to the general steady-flow potential equation. The small parameter in terms of which the series is written, although undefined, could be inferred to be of the order of the relative change in the cross-sectional area between the channel exit and the throat. The coefficients consist of polynomials in y^2, each power of which is multiplied by an arbitrary function of x, where x and y are coordinates in the longitudinal and transverse directions respectively. The new and important feature of this solution was that arbitrary wall shapes could be considered; at each order of approximation the governing equations and boundary conditions give equations which determine the unknown function of x in the polynomial solution. However, neither the conditions under which this solution holds nor its relation to the previously mentioned similarity solutions was considered, although it appeared that the region of validity of the solutions was not limited in the x direction. An extension to flows with shock waves was also presented (ref. 7).

It was shown later (ref. 8) that the Szaniawski series could be derived in a systematic fashion using asymptotic methods, that this solution should be considered as an outer solution which might not remain uniformly valid as a sonic throat was approached, and finally, that there exists an inner region about the throat, in which the aforementioned similarity regions could hold. More importantly, it was shown in this derivation that in the outer region, where x and y are of the same order, the governing

equations for each order of approximation are linear, so that solutions for flows with arbitrary wall shapes are easily found; again, it is only in a very thin throat region that the nonlinear equation need be considered. In reference 8, inner and outer solutions were matched and it was demonstrated that unsteady flows could be analyzed using the same asymptotic methods; no shock waves were considered. Finally, in reference 9 a steady flow with a shock wave was considered and it was demonstrated that another inner region enclosing the shock wave was necessary, since solutions immediately downstream of the shock wave do not match with channel-flow solutions at that location. Applications to unsteady flows with shock waves were outlined in reference 10. The extension of these ideas to cover many different steady and unsteady transonic internal flows is described in the following sections.

2. PERTURBATION PROCEDURES

An analytical description of two- and three-dimensional, steady and unsteady, transonic channel and cascade flows requires introduction of an intimidating variety of nondimensional parameters. A few of these parameters are numerically small, and one is led to consider the possibility of deriving asymptotic solutions which are expected to be valid in some limit as these parameters approach zero. In selecting appropriate limiting cases for study, it is necessary to make choices about the relative orders of magnitude of the small parameters. One dimensionless quantity, say ε, is identified as the basic small parameter, and then various cases can be studied depending on the orders of magnitude of the other parameters relative to ε, in the limit as $\varepsilon \to 0$. Although the number of parameters is thereby reduced only by one, it is often possible to obtain analytical solutions and thus to show the dependence on the remaining parameters explicitly. In principle these solutions can be carried out to higher order, to provide numerical accuracy over a wider parameter range.

Many of the examples to be considered are concerned with two-dimensional transonic flow through a converging-diverging channel with small area change, typically with a shock wave in the diverging part. A steady flow is characterized by two nondimensional small parameters, which measure the relative change in channel cross-section area and the typical difference between the local flow Mach number and one. The width and length of the channel are taken to be of the same order, and a parameter ε^2 is introduced as a measure of the area change. If the flow is to accelerate through sonic speed at the throat (choked flow), the Mach number M_∞ in the undisturbed flow ahead of the channel is given by $1 - M_\infty = O(\varepsilon)$; an area change $O(\varepsilon^2)$ then gives a change $O(\varepsilon)$ in Mach number.

Unsteady motions might be caused by oscillations of the channel walls or by oscillations in the downstream pressure. If the motion is caused by wall oscillations, one additional small parameter is the nondimensional amplitude α of the wall oscillations. A second new parameter which may be small is the reduced frequency $\tau^{-1} = \omega L/a^*$, where L is the channel half-width, ω is the angular frequency, and a^* is the critical sound speed in the undisturbed flow. Thus τ^{-1} is proportional to the ratio of the flow residence time to the period of the impressed oscillations. Asymptotic solutions can be derived for $\varepsilon \to 0$, $\tau^{-1} \to 0$, and $\alpha \to 0$, corresponding to selected relationships for the orders of magnitude of τ^{-1} and α in terms of ε.

Since nondimensional velocity changes are $O(\varepsilon)$, the entropy change across a shock wave is $O(\varepsilon^3)$. If a shock wave is present and is nearly plane, the nondimensional vorticity is smaller than $O(\varepsilon^3)$, and a velocity potential can be used to describe the first few terms in asymptotic expansions of the flow variables. If the coordinates are made nondimensional with L, the time with ω^{-1}, and speeds with a^*, the full potential equation is

$$a^2 \nabla^2 \phi - \vec{q} \cdot \nabla \frac{q^2}{2} - \frac{2}{\tau} \vec{q} \cdot \vec{q}_t - \frac{1}{\tau^2} \phi_{tt} + \frac{1}{\tau} F'(t) = 0 \qquad (2.1)$$

where

$$F(t) = \frac{1}{\tau} \phi_t + H = \frac{1}{\tau} \phi_t + \frac{1}{2} q^2 + \frac{a^2}{\gamma - 1} \qquad (2.2)$$

Here H is the nondimensional total enthalpy and $a^2 = p/\rho$, where the sound speed a, the pressure p, and the density ρ have been made nondimensional with the corresponding critical values in the undisturbed flow. Upstream of a shock wave $F(t) = H_\infty = (1/2)(\gamma+1)/(\gamma-1)$, and F(t) has the same value downstream if the flow is steady. Across a moving shock wave defined by $S(x,y,t) = 0$, the jump in H is given by

$$H_d - H_u = c\,(q_{nd} - q_{nu}) \qquad (2.3)$$

where x, y are coordinates along and normal to the undisturbed flow direction, with $x = 0$ at the channel throat and $y = 0$ along the channel center line; $q_n = \vec{q} \cdot \nabla S/|\nabla S|$ is the velocity component normal to the shock wave; $c = -\tau^{-1} S_t/|\nabla S|$ is the shock speed; and the subscripts u, d refer to conditions immediately upstream and downstream of the shock. The Prandtl relation at the shock wave gives

$$(q_{nu} - c)(q_{nd} - c) = \{H_\infty - c\,(q_{nu} - c/2)\}\{2\,(\gamma-1)/(\gamma+1)\} \qquad (2.4)$$

For a symmetric channel the walls are given by

$$y_w = \pm \{1 - \varepsilon^2 f(x) + \alpha G(x,t)\} \qquad (2.5)$$

(if wall oscillations, when present, also are symmetric), and the boundary condition at the walls is

$$v_w = \tau^{-1} \partial y_w/\partial t + u_w \partial y_w/\partial x \qquad (2.6)$$

where $u_w = u\,(x,y_w,t)$ and $v_w = v\,(x,y_w,t)$.

Throughout most of the channel the perturbations from a uniform flow at the critical sound speed are described by a perturbation potential ϕ. In the cases to be considered, ϕ can be expanded in the form

$$\phi = \varepsilon \phi_1(x,t) + \varepsilon^2 \phi_2(x,y,t) + \varepsilon^3 \phi_3(x,y,t) + \ldots \qquad (2.7)$$

where it has been anticipated that the first term describes a one-dimensional flow and that two-dimensionality appears in the second approximation. As discussed later, it can be shown that this kind of representation fails in thin regions immediately behind a shock wave and at a channel entrance or exit, and in a different way close to the throat. The approximate pressure can be found, if only terms larger than $O(\varepsilon^3)$ are needed, by expanding the isentropic relation $p = a^{2\gamma/(\gamma-1)}$. The leading terms are

$$p = 1 - \varepsilon \gamma \phi_{1x} - \varepsilon^2 \gamma \phi_{2x} - \gamma \varepsilon \tau^{-1} \phi_{1t} + \ldots \qquad (2.8)$$

provided that a term proportional to $F(t) - H_\infty$ can be neglected; this term is $O(\alpha)$, as noted below.

The shock-wave position $x = x_s(y,t)$ is expanded, for the cases considered here, in the form

$$x_s(y,t) = x_{so}(t) + \varepsilon x_{s1}(t) + \ldots \qquad (2.9)$$

where it has been anticipated that in most applications the first two terms will be independent of y; typically it is found that $\partial x_s/\partial y = O(\varepsilon^{3/2})$. For unsteady flows, the shock-wave motion is found to be quasi-steady for frequencies low enough that $\tau^{-1} << \varepsilon^2$, and the time required for disturbances from the channel exit to reach the shock wave is short in comparison with one period when $\tau^{-1} << \varepsilon$. Thus two important special cases arise for $\tau^{-1} = O(\varepsilon^2)$ and $\tau^{-1} = O(\varepsilon)$; these will be referred to as "low" and "moderate" frequencies in the following. The wall oscillations with amplitude $O(\alpha)$ are equivalent to time-dependent area changes $O(\alpha)$, which imply changes $O(\alpha/\varepsilon)$ in the flow velocity; α is taken to be at most $O(\varepsilon^2)$. For τ^{-1} equals $O(\varepsilon^2)$ or larger, the shock wave velocity is also $O(\alpha/\varepsilon)$, and so the shock-wave displacement is $O(\tau\alpha/\varepsilon)$. Thus the amplitude of the shock-wave oscillation is O(1) if $\alpha = O(\varepsilon\tau^{-1})$ and small if $\alpha << \varepsilon\tau^{-1}$. It now also can be seen, from equations (2.2) and (2.3), that the neglected term proportional to $F(t) - H_\infty$ in equation (2.8) is $O(\alpha)$.

In the three-dimensional examples to be considered, the variation of Mach number is taken to be $O(\varepsilon)$ in a transverse direction as well as in the flow direction. For a cascade the blade stagger, as well as the ratio of spacing to chord, is taken to be O(1). In one example of unsteady supersonic channel flow, the ratio of channel length to width is $O(\varepsilon^{-1/2})$; although boundary layers are thin, the displacement thickness due to separation bubbles in this example is of the same order as the variation in channel width. The viscosity in general is taken to be small enough that the shock-wave thickness is small in comparison with any relevant streamwise length; in cases where shock-wave structure is considered, the Reynolds number is such that the shock-wave thickness is $O(\varepsilon)$.

3. STEADY FLOWS

Two-dimensional Inviscid Channel Flow

To provide an introduction for applications to other flows, the results of reference 9 are summarized here, with some minor changes in notation. Substitution of the expansion (2.7) into the potential equation (2.1) and boundary condition (2.6) leads to a first approximation defined by

$$\phi_{1yy} = 0 \ , \qquad \phi_{1y}(x,\pm 1) = 0 \qquad (3.1)$$

The solution has the form $\phi_1 = \phi_1(x)$, as already anticipated in (2.7). The second approximation is defined by

$$\phi_{2yy} = (\gamma+1)\,\phi_{1x}\,\phi_{1xx} \ , \qquad \phi_{2y}(x,\pm 1) = \mp f'(x) \qquad (3.2)$$

With the further requirement that the flow be choked, so that $\phi_{1x}(0) = 0$, for $f'(0) = 0$, the solution for ϕ_1 can be completed:

$$\phi_{1x}(x) = \pm \left(\frac{2}{\gamma+1}\right)^{1/2} \{f(0) - f(x)\}^{1/2} \qquad (3.3)$$

If $f = 0$ at the channel entrance and the undisturbed velocity $u = u_\infty$ is expanded as $u_\infty = 1 + \varepsilon u_{1\infty}$

$+ \varepsilon^2 u_{2\infty} + \ldots$, the constant f(0) is related to $u_{1\infty}$ by (for subsonic incoming flow) $u_{1\infty} = - \{2f(0)/(\gamma+1)\}^{1/2}$.

The solution for ϕ_2 contains a function $h_2(x)$ that is still unknown:

$$\phi_2(x,y) = \frac{1}{2} f'(x) \left(\frac{1}{3} - y^2 \right) + h_2(x) \tag{3.4}$$

The differential equation and boundary condition for the third approximation then allow completion of the solution for the second approximation. The function $h_2'(x)$ is found to be

$$h_2'(x) = (3 - 2\gamma) \phi_{1x}^2/6 + c_2/\{(\gamma+1)\phi_{1x}\} \tag{3.5}$$

where the constant c_2 is discontinuous at a shock wave. For choked flow, $c_{2u} = 0$. The Prandtl relation (2.4) gives

$$u_{1u} + u_{1d} = 0 \ , \qquad u_{2u} + u_{2d} = - u_{1u} u_{1d} \tag{3.6}$$

where $u_1 = \phi_{1x}$ and $u_2 = \phi_{2x}$. A tentative result $c_{2d} = - 2\gamma(\gamma+1) u_{1u}^3/3$ can be found by integrating the condition for u_{2d} across the channel, from y = -1 to y = 1. It is evident, however, that the solution for ϕ_2 can only satisfy the Prandtl relation in such an averaged sense. The difficulty arises because the small shock-wave curvature implies a streamline curvature that is inconsistent with the wall curvature, and so the solution (3.4) is not complete immediately behind the shock wave. To satisfy both the shock relations and the wall boundary condition an "inner" solution satisfying a Prandtl-Glauert equation is needed for $x - x_{so} = O(\varepsilon^{1/2})$. The correction to be added to the expansion (2.7) is found to be

$$- \varepsilon^{5/2} f''(x_{so}) (4/\pi^3) \sum_{n=1}^{\infty} (-1)^n n^{-3} \exp(-n\pi X) \cos n\pi y \tag{3.7}$$

where $X = \{(\gamma+1)u_{1u}\varepsilon\}^{-1/2} (x-x_{so})$. As the intersection of the shock wave and the wall is approached, the series can be summed to show explicitly the expected logarithmic singularity in the pressure gradient. Also it can now be verified, by an integral condition expressing mass conservation, that c_{2d} has the value anticipated above. Although needed to provide the flow details near the shock wave, this inner solution is not, therefore, really required for the evaluation of c_{2d}. The analogous correction for axisymmetric flow was also given in reference 9.

At the channel entrance and exit, an expansion of the form (2.7) in general will not match with solutions in the external flow, and a Prandtl-Glauert equation is again needed for a distance $\Delta x = O(\varepsilon^{1/2})$; an example will be shown later. Near the channel throat, within a short distance $x = O(\varepsilon)$, the terms ϕ_{yy} and $(\gamma+1)\phi_x \phi_{xx}$ in the potential equation are of the same order of magnitude. For the case of acceleration from subsonic to supersonic speed, if $f''(0) = - 1$, the first approximation to the solution has the simple polynomial form

$$\phi = \varepsilon^3 \frac{1}{2} (\gamma+1)^{1/2} \left\{ \frac{x^2}{(\gamma+1)\varepsilon^2} + \frac{x}{(\gamma+1)^{1/2}\varepsilon} \left(y^2 - \frac{1}{3} \right) + \frac{y^2}{6} \left(\frac{y^2}{2} - 1 \right) \right\} \tag{3.8}$$

Although this expression should, strictly speaking, be obtained as a solution of the nonlinear equation $\phi_{yy} = (\gamma+1)\phi_x \phi_{xx}$, it is actually seen to contain just the largest terms in the Taylor expansion, about x = 0, of the solution $\varepsilon\phi_1 + \varepsilon\phi_2$ given above. In other circumstances, if the flow is not quite choked

or if a shock wave is present very close to the throat, a special formulation for $x = O(\varepsilon)$ and/or for $x = O(\varepsilon^{1/2})$ may be essential, as noted in references 5, 8, 9, 16, and 17.

Cascade Flows

A limiting case of transonic cascade flow has been studied in reference 11. The ratio of blade spacing to blade chord length is O(1); the stagger angle $\tan^{-1}\lambda = \tan^{-1}(d/\upsilon) = O(1)$, where υ = blade spacing and $d = \lambda\upsilon$; the blade thickness, camber and angle of attack are $O(\varepsilon^2)$; and for high subsonic speeds ahead of the cascade the Mach number M_∞ is expressed by $M_\infty^2 = 1 - K\varepsilon$. There is then a region analogous to a channel in which a nearly one-dimensional flow is described by an asymptotic expansion of the form (2.7). Ahead of the cascade, however, the largest flow perturbations are two-dimensional. As for an isolated airfoil the length scale in a transverse direction is $O(\varepsilon^{-1/2})$. On this larger scale the spacing between the blades appears very small, and in the limit the flow is the same as the flow past a scalloped wall, as sketched in figure 1. Since the "outer" solutions do not match directly to the "channel" solutions, additional solutions are needed near the leading edges, and likewise near the trailing edges. Here y = O(1) and the length scale in the x-direction is $O(\varepsilon^{1/2})$, so that an "edge" solution describes the flow in a thin strip transverse to the flow and containing one of the edges; a similar situation arises at trailing edges. These edge regions are indicated in figure 1.

The outer solution has the form

$$\phi = \varepsilon^{3/2}\tilde{\phi}_{3/2}(\tilde{x},\tilde{y}) + \varepsilon^2\tilde{\phi}_2(\tilde{x},\tilde{y}) + \ldots \tag{3.9}$$

where $\tilde{x} = x$, $\tilde{y} = \varepsilon^{1/2}K^{1/2}(y - \lambda x)$. The upper and lower blade surfaces are $y = \varepsilon^2 f_u(x)$ and $y = \varepsilon^2 f_\upsilon(x)$, respectively. If it is required that there be no mass flow $O(\varepsilon^2)$ around the leading edges, it is found (ref. 11) that the velocity in the leading-edge regions remains $u = 1 + \varepsilon u_{1\infty} + \ldots$, as in the undisturbed flow, and that the first term in the angle of attack has a specific value, such that $\alpha = \varepsilon^2 f_u(d)/d + \ldots$. The expansion of α in terms of ε then has the form

$$\alpha = \varepsilon^2 f_u(d)/d + \varepsilon^{5/2}\alpha_{5/2} + \ldots \tag{3.10}$$

For parabolic surfaces a complex perturbation velocity is found to be

$$\tilde{\phi}_{3/2\tilde{x}} - i\tilde{\phi}_{3/2\tilde{y}} = -\Delta_u/(K^{1/2}\pi)\ln(1 - e^{2\pi i\tilde{z}/d}) \tag{3.11}$$

where $\tilde{z} = \tilde{x} + i\tilde{y}$ and $\Delta_u = f_u'(d) - f_u'(0)$.

Near the edge x = d the potential has the form

$$\phi = \varepsilon^2(\upsilon/\pi)\hat{\phi}_2(\hat{x},\hat{y};\varepsilon) + \ldots \tag{3.12}$$

where $\hat{x} = \pi(x - d)/\{(\varepsilon K)^{1/2}\upsilon\}$, $\hat{y} = \pi(y - \upsilon)/\upsilon$ and matching with the outer solution shows that $\hat{\phi}_2 = O(\ln\varepsilon)$ as $\varepsilon \to 0$. A conformal transformation $\hat{x} + i\hat{y} = \zeta - 1 - \ln\zeta$ maps the local flow onto the upper half of the ζ-plane. The complex perturbation velocity is

$$\hat{\phi}_{2\tilde{x}} - i\hat{\phi}_{2\tilde{y}} = \frac{\Delta_u}{\pi}\left\{\frac{\zeta}{\zeta-1}\ln\frac{d/\upsilon}{2(\varepsilon K)^{1/2}} - \ln(\zeta-1)\right\} + \frac{\Delta_d}{\pi}\left\{\frac{1}{\zeta-1} + \ln\frac{\zeta-1}{\zeta}\right\}$$

$$+ \frac{d\alpha_{5/2}}{\upsilon K^{1/2}(\zeta-1)} - i f_u'(0) + i\frac{f_u(d)}{d} \qquad (3.13)$$

where $\Delta_d = f_u'(d) - f_\upsilon'(0)$. It can be shown that this result matches properly with the channel and outer solutions. Analogous inner solutions are needed for thin regions containing the trailing edges.

At low supersonic speeds, such that $M_\infty^2 = 1 + K\varepsilon$, the flow ahead of a cascade in terms of coordinates $\tilde{x}$ and $\tilde{y}$ is again equivalent to the flow past a scalloped wall. For $\tilde{y} = O(1)$ the characteristics and the weak shock waves from the leading edges can still be considered parallel. Here the first approximation is given by the linear wave equation of supersonic small-disturbance theory. At larger distances disturbances from the forward part of a blade will overtake the shock wave from the leading edge of that blade, whereas disturbances further to the rear are overtaken by the shock from the next blade. A limiting characteristic separates these disturbances and extends to infinity. This effect becomes important for $y = O(\varepsilon^{-1})$, i.e., $\tilde{y} = O(\varepsilon^{-1/2})$, where a nonlinear far-field description is required. The solution gives an "N-wave" for the pressure and shows that the shock-wave strength is $O\{(\varepsilon y)^{-1}\}$ as $\varepsilon y \to \infty$. The flow inclination angle approaches a value which remains constant along the limiting characteristic and which is found to equal the average blade slope between $x = 0$ and $x = d$, namely $\varepsilon^2 f_u(d)/d$. Thus the flow far ahead of the cascade is affected and has a prescribed "unique incidence angle" equal to the value $\varepsilon^2 f_u(d)/d$ at the limiting characteristic; a second approximation to this value can also be derived.

Three-Dimensional Flows

Three-dimensional flow through a transonic compressor rotor has been studied (refs. 12, 13) as an extension to the cascade flow presented in reference 11. The problem has an additional small parameter δ which orders the difference between the undisturbed velocity relative to a moving blade and sonic velocity. If velocities are made dimensionless with respect to the sonic velocity in the undisturbed flow and lengths by the ratio of this sonic velocity to the constant angular velocity, then the dimensionless undisturbed velocity relative to the blade U_o is

$$U_o^2 = R^2 + M_{oa}^2 \qquad (3.14)$$

where, because of the way in which lengths are nondimensionalized, R is both the dimensionless radius and the tangential component of the velocity relative to the blade. The Mach number of the undisturbed axial flow is M_{oa}; i.e., the incoming flow in absolute (engine- or laboratory-fixed coordinates) terms is in the axial direction with no swirl or radial component. Since U_o is a Mach number, the radius R_{so} at which the relative Mach number is one is $R_{so}^2 = 1 - M_{oa}^2$ and $U_o^2 = 1 + R^2 - R_{so}^2$. Hence, if $\delta = O(U - 1) = O(R - R_{so})$ then a stretched radial coordinate z can be defined and U_o written in terms of z and δ as follows:

$$z = \frac{R - R_{so}}{\delta} \tag{3.15a}$$

$$U_o^2 = 1 + 2\delta R_{so} z + \delta^2 z^2 \tag{3.15b}$$

As in the cascade-flow problem the thickness of the blades is taken to be $O(\varepsilon^2)$. Then, in the channel-like part of the flow between the blades, the perturbation to the flow velocity is $O(\varepsilon)$, again just as in the cascade or two-dimensional channel-flow problems. It is seen, then, that the various physical problems which can be considered are characterized mathematically by the relative orders of δ and ε. For $\delta << \varepsilon$, the flow is dominated by the constriction provided by the channel with very little effect due to the shear in the incoming undisturbed flow U_o; the flow is essentially two-dimensional with three-dimensional effects relegated to higher-order terms. For $\delta >> \varepsilon$, the inverse is true in that the flow is dominated by the incoming shear flow and effects of the side walls or blades arise only in higher-order terms. For $\delta = O(\varepsilon)$, however, both shear and flow constriction effects are of equal importance and the interplay between them most pronounced. It is this case which is considered in references 12 and 13.

A model problem consisting of a shear flow in a three-dimensional channel with blade-like flow constrictions on opposing walls was studied first (refs. 14, 15). The flow field considered is similar to that through an axial-flow rotor with zero stagger angle. Solutions are presented both for $\delta = O(\varepsilon)$ and $\delta >> \varepsilon$. In the more interesting case, $\delta = O(\varepsilon)$, it is shown that just as for two-dimensional nozzle flows, there are limits on the average Mach number which can occur in the entrance flow when choking occurs at the minimum area. That is, for isentropic flow through a nozzle with a given area ratio, there are two Mach numbers at the nozzle entrance for which sonic velocity occurs at the throat, one supersonic and one subsonic. In the problem under consideration, this same result is found only for average (across the span) Mach numbers; this then has consequences on the allowable positions for the sonic surface in the incoming flow. In addition to this similarity to one-dimensional flow interpretations, it is demonstrated that when a shock wave occurs downstream of the minimum area, the main effect of a variation in back pressure is to change the shock location. This is true even when, because of the fact that the flow is a shear flow, the shock wave fills only part of the channel. In that event, variations in back pressure do indeed change the shape of the shock wave and because signals can move through the subsonic flow beneath the wave, the flow upstream of the wave is affected. However, the upstream influence of these pressure signals is limited to a distance $O(\varepsilon^{1/2})$ upstream of the shock wave; the essential result of changes in back pressure is a change in location of the wave. Finally, it is shown that for $\delta >> \varepsilon$, the analogy with one-dimensional flows breaks down. For example, the Mach number at which bifurcation in solutions occurs is not unity as it is in the case when $\delta = O(\varepsilon)$.

The formulation of the problem of transonic flow through a compressor rotor follows that of the cascade (two-dimensional) flow quite closely. Thus, at a constant radius, the flow appears to be that through a cascade with the added feature that as the span of the blades is traversed, the stagger angle changes. However, the fact that the flow is three-dimensional causes several fundamental differences as might be expected.

The limit process chosen is important because it sets the physical problem considered. As mentioned previously $\delta = O(\varepsilon)$ is the case considered, but it remains to relate δ to a physical quantity. In references 12 and 13, with $\delta = O(R - R_{so})$ and since $R - R_{so}$ is of the order of the blade span, then δ is chosen to be of the order of the (dimensionless) blade chord and in particular the constant axial

component of the blade chord at the hub C_a. Since $(R - R_{so})/\delta = 0(1)$, this assumes that in the limit $\varepsilon \to 0$, so $\delta \to 0$, the blade aspect ratio remains unchanged. To ensure that the complete channel geometry remains unchanged in the limit, the dimensionless blade spacing at the tips, scaled with respect to C_a, is also taken to be O(1). Thus, if R_t is the dimensionless tip radius and B the number of blades,

$$s \equiv \frac{2\pi R_t}{B C_a} \tag{3.16}$$

Thus $B^{-1} = O(C_a)$ and in the limit as $\varepsilon \to 0$, $B \to \infty$ to retain the proper geometric properties during the limit process. The limit process $B^{-1} \to 0$ has been used in other asymptotic analyses of cascade flow.

It is necessary to consider the same regions as in the cascade problem, as pictured in figure 1. Indeed in the far field, the boundary of which is again a scalloped wall as in figure 1a, the flow is two-dimensional to lowest order. Because, as indicated in equation (3.15b), the flow is expanded about sonic conditions, at which z = 0, the distance between corners (edges) is independent of radius to lowest order. This distance is, of course, dependent upon the radius and so there is an error at any order of approximation when an expansion is employed. It can be shown that this error is not cumulative as one passes from one edge to the next. The same small error is made at each edge.

To the order desired, the perturbations to the incoming velocity may be written in terms of a velocity potential. In the channel, the lowest-order term is $O(\varepsilon)$, with higher-order terms proceeding in powers of $\varepsilon^{1/2}$. A coordinate system is chosen such that for a given blade x is measured along the helical line formed by those streamlines of the undisturbed relative flow which pass through the radius associated with the leading edge of the blade. A coordinate y is defined, locally perpendicular to x, which is constant along the surface formed by an infinitesimally thin blade at zero angle of attack; the blade shape is defined relative to this surface. Finally, z is defined in equation (3.15a) as being measured along a radius. Transformations of the governing equation to these variables results in a problem description quite similar to that for flow through a three-dimensional channel (refs. 14, 15) or a cascade (ref. 11).

In the channel, $\phi_1 = \phi_1(x)$ and $\phi_{3/2} = \phi_{3/2}(x)$, with both y and z dependence being given in ϕ_2 (x, y, z); hence, in general, this follows the results found for the cascade. Also, outer far-field solutions ahead of the rotor have the form shown in equation (3.9) with the exception that $\tilde{\phi}_2 = \tilde{\phi}_2(\tilde{x}, \tilde{y}, \tilde{z})$. Indeed, the cascade solutions for $\tilde{\phi}_{3/2}$ may be used. As $\tilde{y} \to 0$, for $0 < x < d$ (notation in figure 2), the resulting relations for $\tilde{\phi}_{3/2}$ and $\tilde{\phi}_2$ are those found for y = O(1) and $0 < x < d$; i.e., they match. In addition, the terms $\alpha_{5/2}$ and α_2 in the expansion for the angle of attack have similar forms. However, in the leading-edge region, the flow is three-dimensional to lowest order; in equation (3.12), $\hat{\phi}_2 = \hat{\phi}_2(\hat{x}, \hat{y}, \hat{z}; \varepsilon)$, so cascade solutions do not suffice. Because the governing equation for $\hat{\phi}_2$ is linear, the combination $\hat{\phi}_2 = \hat{\phi}_{2c}(\hat{x}, \hat{y}; \varepsilon) + \hat{\phi}_2^*(\hat{x}, \hat{y}, \hat{z}; \varepsilon)$ is employed, where $\hat{\phi}_{2c}$ is the cascade solution with velocity components as shown in equation (3.13). This is convenient because the cascade solution matches with both the outer solution and the lowest-order channel solution, so the solution for ϕ_2^*, which must be found numerically, is simpler. The governing equation for ϕ_2^* is

$$\frac{z}{z_a}\,\phi^*_{2\hat{x}\hat{x}} + \phi^*_{2\hat{y}\hat{y}} + \frac{1}{\pi^2 B_o^2}\,\phi^*_2 = -\left(\frac{z}{z_a} - 1\right)\phi_{2c\hat{x}\hat{x}} \tag{3.17a}$$

$$B_o = \frac{R_t}{S\,M_{oa}\,R_{so}} \tag{3.17b}$$

$$z_a = \frac{z_t + z_h}{2} \tag{3.17c}$$

$$\hat{x} = \frac{\pi d_o}{\varepsilon^{1/2}\hat{C}}\left(\frac{x}{d} - 1\right) \tag{3.17d}$$

$$C^2 = \frac{-2m\,z_a}{B_o^2} \tag{3.17e}$$

where the subscripts t and h refer to tip and hub conditions respectively and d_o is the lowest-order term in the expansion for d. Equation (3.17a) is a very simple form of equation for mixed flow. It can be shown that for $z_a < 0$ (sonic conditions at $z = 0$) the average Mach number is subsonic and for $z_a > 0$ it is supersonic. Thus if $z_a < 0$, then for $z < 0$ the flow is subsonic and equation (3.17a) is elliptic, whereas for $z > 0$ the flow will be supersonic and equation (3.17a) is hyperbolic. Since z_t is the largest value of z, the problem considered depends upon the Mach number at the blade tip. In the numerical solutions mixed Dirichlet and Neumann boundary conditions are used with the normal derivatives all being zero and $\phi = 0$ being the condition used as $x \to -\infty$ for all y.

In the trailing-edge and downstream outer and far-field regions, expansions and methods of solution similar to those described for the leading edge are employed, with one additional feature. A vortex sheet starts at the trailing edge of each blade and extends downstream to infinity; in keeping with the fact that the solution found is for lightly loaded blades, these vortex sheets remain on planes y = constant. The pressure (and hence u_1) and $v_{3/2}$ are continuous across these sheets and so the jump $\Delta\phi$ across each sheet is constant, independent of x. However ϕ_z is not continuous across the sheet. It is this fact which differentiates the solution for three-dimensional flow from that for the cascade. In cascade flow ϕ is discontinuous across surfaces extending downstream from the trailing edges, but only two-dimensional velocity components are desired and they are continuous. In the three-dimensional flow, there is a spanwise variation in circulation and hence in $\Delta\phi$, and ϕ_z is discontinuous across the sheet. The net result is that a periodic discontinuous solution for ϕ is introduced in the trailing-edge and outer and far-field regions.

Solutions in the various regions are used to form composite solutions. Typical results are shown in figure 3, in which lines of constant Mach number at a given radial position and pressure distributions on the suction side of a blade are shown for a typical case when the tip Mach number is subsonic. Details are found in references 12 and 13.

Solutions for the case where the tip Mach number is supersonic were attempted. The numerical solution of equation (3.17a) in the leading- and trailing-edge regions involves mixed hyperbolic (for $z > 0$) and elliptic (for $z < 0$) flow, with given solutions to which these inner solutions must match for all z. The problem does not appear to be improperly posed since it is mixed; however, convergence to a solution has not been obtained. When the downstream matching condition is removed in the

hyperbolic region, and additional conditions imposed upstream, little improvement is seen. To date, a solution to this problem has not been found.

An interesting result found from these studies is the aforementioned fact that far from the rotor, the flow is two-dimensional to lowest order, for both subsonic and supersonic tips. Thus, if the average Mach number of the undisturbed flow is supersonic, the two-dimensional wave equation holds, while if it is subsonic, the Laplace equation governs the flow. The flow in the leading-edge region is three-dimensional. Hence, it appears that shock waves, which originate at the leading edge of a blade for $z > 0$ and reflect off the outer shroud to the sonic surface and back many times, eventually coalesce in such a way as to form a two-dimensional wave at the average Mach number of the undisturbed flow, if it is supersonic, and do not coalesce into any recognizable wave if the average Mach number is subsonic. Further work on this problem is needed.

4. UNSTEADY FLOWS

"Low" Frequencies

For "low" reduced frequencies $\tau^{-1} = O(\varepsilon^2)$, say $\tau^{-1} = k\varepsilon^2$, the solution (3.3) for ϕ_{1x} remains unchanged, a function only of x. If the channel walls oscillate with amplitude $\alpha << \varepsilon^3$, or the fluctuations in exit pressure p_b are small in comparison with ε^2, the term h_2 in the solution (3.4) for ϕ_2 is still independent of t, and the first approximation x_{so} to the shock-wave position (2.9) likewise remains independent of t. But for $\alpha = O(\varepsilon^3)$, or for changes $O(\varepsilon^2)$ in p_b, h_2 does depend on t, and equation (3.5) is replaced by (refs. 16,17)

$$h_{2x}(x,t) = (3 - 2\gamma)\,\phi_{1x}^2/6 + \{c_2(t) + G(x,t)\}/\{(\gamma+1)\,\phi_{1x}\} \tag{4.1}$$

where now

$$c_{2u}(t) = -G(0,t) \tag{4.2}$$

$$c_{2d}(t) = c_{2d}^{(s)} + G_d(t) - G(x_1,t) \tag{4.3}$$

Here $x = x_1$ is the location of the channel exit; $c_{2d}^{(s)}$ is the steady-state value of c_{2d}; and $G_d(t)$ is proportional to an unsteady term in the exit pressure, which in some examples is prescribed as a boundary condition. The first approximation x_{so} to the shock position (2.9) is now a function of time; i.e., the shock-wave displacement is now O(1). Again an inner solution is needed just downstream of the shock wave to complete the description of the flow, but not for the calculation of c_{2d}. This solution is now written for $x - x_{so}(t) = O(\varepsilon^{1/2})$, so that the coordinate X in equation (3.7) is measured relative to the instantaneous shock-wave position. The potential near the throat again has the form (3.8), but with x replaced by $x + \varepsilon G_x$, again for $f''(0) = -1$. The shape of the sonic line is then found by setting $\phi_{1x} = 0$.

The Prandtl relation (2.4) leads to a nonlinear ordinary differential equation for x_{so}:

$$\frac{dx_{so}}{dt} = -\frac{1}{4ku_{1u}}\left\{\frac{2}{3}\gamma(\gamma+1)\,u_{1u}^3 + N(t)\right\} \tag{4.4}$$

where $N(t) = c_{2d}(t) - c_{2u}(t)$. For a simple example, the channel walls are taken to have the parabolic

form $f(x) = \{(\gamma+1)\, u_{1\infty}^2/2\}\{1 - (x/x_1)^2\}$ for $-x_1 < x < x_1$, with periodic forcing expressed by $G(x_1,t) - G(0,t) - G_d(t) = \beta \sin t$, where β = constant. Then $\phi_{1x} = \pm |u_{1\infty}\, x/x_1|$ and

$$\frac{dx_{so}}{dt} + \frac{\gamma(\gamma+1)\, u_{1\infty}^2}{6\, k\, x_1^2}\left(x_{s0}^2 - \frac{x_{so}^{(s)^3}}{x_{so}}\right) = \frac{\beta\, x_1}{4\, k\, |u_{1\infty}|\, x_{so}} \sin t \qquad (4.5)$$

The shock-wave motions are identical for a case with stationary walls and oscillating back pressure such that $G_d(t) = -\beta \sin t$ and for a case in which the back pressure is constant and the walls oscillate in pitch with $G(x,t) = \beta(x/x_1) \sin t$. (The notation again is slightly different from that of the original references.)

For this example the singular points of the differential equation (4.4) are saddle points and centers located periodically along the time axis (i.e., along $x_{so} = 0$). The integral curves show two quite different types of behavior (ref. 16) depending on whether or not the integral curve from a saddle point later returns to $x_{so} = 0$; in a dividing case, the integral curve joins successive saddle points. The different cases are sketched in figure 4. In case (a) the shock wave periodically disappears upstream, reappears at the throat, moves a limited distance downstream and then again accelerates upstream through the throat. In case (c) the motion approaches a specific periodic motion unless the shock wave is initially too close to the throat. The pattern changes from c) to b) to a) as the amplitude of oscillation increases, or as the frequency decreases, or as the back pressure increases (such that the steady-state shock position moves upstream).

The shock-wave position in a numerical example corresponding to case (a) of figure 2 is shown in figure 5. It is seen that the shock disappears upstream at a particular time $t = t_*$. The details of the motion through the throat and the upstream part of the channel can be studied in terms of suitable shorter time scales. In a time interval $t - t_* = O(\varepsilon)$ the shock-wave speed $\tau^{-1}\, dx_s/dt$ has increased from $O(\varepsilon^2)$ to $O(\varepsilon^{3/2})$, and an implicit solution can be derived for the shock position $x_s = O(\varepsilon^{1/2})$. The time required for passage through this region is found to be $O(\varepsilon \ln \varepsilon)$. In the upstream part of the duct the shock speed is $O(\varepsilon)$. Composite representations for dx_s/dt in terms of x_s were constructed in references 16 and 17. For the special case of parabolic walls, these results can be combined into a single expression for the shock-wave speed:

$$k\,\varepsilon^2 \frac{dx_s}{dt} = -\frac{1}{6}\varepsilon^2\, \gamma(\gamma+1)\, u_{1\infty}^2\, \frac{x_s^2}{x_1^2} + \frac{1}{4}\varepsilon^{3/2}(\gamma+1)\, |u_{1\infty}| \left\{ \frac{x_s}{\varepsilon^{1/2}\, x_1} - \left[\frac{x_s^2}{\varepsilon\, x_1^2} + \frac{2N(t_*)}{(\gamma+1)\, u_{1\infty}^2} \right]^{1/2} \right\} + \cdots \qquad (4.6)$$

For $x_s = O(1)$ and positive, this result is correct to $O(\varepsilon^2)$ and is consistent with equation (4.4). Elsewhere, for small $|x_s|$ and for $x_s < 0$, the first term on the right side is of higher order than the second term. For $x_s = O(1)$ and negative, the largest part of the second term is proportional to x_s, and integration gives

$$\frac{x_s}{x_1} = -\frac{1}{|u_{1\infty}|}\left\{\frac{N(t_*)}{2(\gamma+1)e}\right\}^{1/2} \exp\left\{\frac{(\gamma+1)|u_{1\infty}|}{2kx_1}\frac{t-t_*}{\varepsilon} - \frac{1}{2}\ln(1/\varepsilon)\right\} \qquad (4.7)$$

for the position of the shock wave as it moves upstream from the throat and then out of the channel at the time when $x_s = -x_1$. The integration constant has been chosen for proper matching with an implicit solution which can be obtained (ref. 17) for $x_s = O(\varepsilon^{1/2})$.

In the periodic flow corresponding to case (c) of figure 4, the largest pressure changes, $O(\varepsilon)$, occur at points which are sometimes ahead of and sometimes behind the shock wave. The phase of the resulting aerodynamic pitching moment depends strongly on the frequency parameter $\tau\varepsilon^2$. This is of particular interest in the case of oscillating walls. For small $\tau\varepsilon^2$, the time lag is small and the moment is nearly in phase with the angular displacement of the walls. For $\tau\varepsilon^2 = O(1)$, there is another component in phase with the angular velocity of the walls, and for large $\tau\varepsilon^2$ this is the only component. If the amplitude α of the wall oscillations is somewhat smaller, so that $\alpha << \tau^{-1}\varepsilon$, the shock-wave equation (4.4) becomes linear and these phase changes can be shown analytically. An especially simple periodic solution is obtained when $\tau\varepsilon^2$ is large (i. e., k is large) and $\tau\alpha/\varepsilon$ is small, again for parabolic walls and for $G(x,t) = \beta\,(x/x_1)\sin t$:

$$\frac{x_{so}}{x_{so}^{(s)}} = 1 - \frac{\beta x_1}{4k|u_{1\infty}|\,x_{so}^{(s)^2}}\cos t \qquad (4.8)$$

where the steady-state position $x_{so}^{(s)}$ has been chosen as the mean position of the shock wave. The shock wave is furthest upstream, giving the largest high-pressure region behind the shock, at the time when the downstream walls have the largest outward velocity.

If the solution (4.8) were regarded as the response to a periodic wall oscillation which starts at time zero, the most obvious choice for an initial condition would be to set $x_s = x_{so}^{(s)}$ at $t = 0$. This choice, however, would give a nonzero mean value for $x_{so} - x_{so}^{(s)}$. Consideration of higher-order terms show more complete differential equation would contain a small term proportional to x_s, and therefore a transient term in the solution with exponential decay that is slow in comparison with the reference time τ. The solution to this initial-value problem thus has zero mean, as in equation (4.8). The same conclusion can be reached in a more systematic way by use of a two-time expansion.

Unsteady transonic flows in asymmetric channels, and in particular in channels with relatively large curvature, have also been studied (ref. 18). In this case, the wall shape is written as $y_w = \pm 1 + \varepsilon f_1(x) \pm \varepsilon^2 f_2(x)$. Thus, the equation for the channel centerline is $y = \varepsilon f_1(x)$ and $\pm(1 + \varepsilon^2 f_2(x))$ are terms which describe walls symmetric about the centerline. Hence ε is a measure of the radius of cuvature of the channel at the throat $x = 0$. The large curvature leads to flow structures and shock-wave shapes very different from those found in symmetric channel flows. Indeed, the shape of the shock wave is found as part of the solution for the inner region immediately downstream of the shock. Only oscillations in back pressure have been considered; details are given in reference 18.

"Moderate" Frequencies

For "moderate" frequencies $\tau^{-1} = O(\varepsilon)$, say $\tau^{-1} = k\varepsilon$, the first time-dependent term in the velocity is $O(\varepsilon^2)$ if the fluctuations in exit pressure are $O(\varepsilon^2)$ or if the channel walls oscillate with amplitude $\alpha = O(\varepsilon^3)$. In this case the function $h_2(x,t)$ in equation (3.4) satisfies the first-order linear partial differential equation

$$2k\,h_{2xt} + (\gamma+1)(\phi_{1x}\,h_{2x})_x = (\gamma+1)(3-2\gamma)\,\phi_{1x}^3/6 + G_x \qquad (4.9)$$

where ϕ_{1x} is once more the known solution (3.3). The characteristics $dx/dt = (\gamma+1)\phi_{1x}/(2k)$ correspond to disturbances traveling upstream relative to the flow, at speed u-a. In the subsonic region behind the shock wave the disturbances of course move upstream toward the shock, whereas in the supersonic region ahead of the shock the disturbances are carried downstream by the flow, also toward the shock wave. The differential equation (4.9) then states that 2k times the rate of change of h_{2x} along the characteristics is equal to the right-hand side, and the solution can then be found by integration along characteristics. Some numerical results are given in reference 19.

For parabolic walls and simple harmonic wall oscillations, expressed for convenience in the exponential form $G(x,t) = \beta\,(x/x_1)\,e^{it}$, analytical solutions for h_{2x} are given by (ref. 17)

$$h_{2x} - \frac{1}{6}\left(\frac{u_{1\infty}}{x_1}\right)^2\left\{(3-2\gamma)\,x^2 - (\gamma+1)\right\} = \frac{\beta\,e^{i(t-\chi)}}{(\gamma+1)\,|u_{1\infty}|\,(1+\upsilon^2)^{1/2}} \qquad x < x_{so} \qquad (4.10)$$

$$= -\frac{c_{2d}^{(s)}\,x_1}{(\gamma+1)\,|u_{1\infty}|\,x} - \left\{1 - \frac{x_1}{x}\exp\left(i\,\upsilon\ln\frac{x}{x_1}\right)\right\}\frac{\beta\,e^{i(t+\chi)}}{(\gamma+1)\,|u_{1\infty}|\,(1+\upsilon^2)^{1/2}} \qquad x > x_{so} \qquad (4.11)$$

where $\nu = \tan\chi = 2k(\gamma+1)^{-1}\,x_1/|u_{1\infty}|$, and it has been assumed that h_{2x} approaches a constant value as $x \to x_1$. The Prandtl relation requires that a term $4k(\gamma+1)^{-1}\,dx_{s1}/dt$ be included in the second of equations (3.6). It follows that

$$\frac{dx_{s1}}{dt} = \frac{\beta\,e^{it}}{4k\,|u_{1\infty}|\,(1+\upsilon^2)^{1/2}}\left\{-2i\sin\chi + \frac{x_1}{x_{so}}\exp\left[i\left(\chi - \upsilon\ln\frac{x_1}{x_{so}}\right)\right]\right\} \qquad (4.12)$$

This result is used later for comparison with a numerical solution of the Euler equations.

If the amplitude of the wall oscillations is increased to $\alpha = O(\varepsilon^2)$, or if the back-pressure fluctuations are $O(\varepsilon)$, the time dependence appears in the first approximation $\phi_1(x,t)$. This case was first discussed in reference 8. Now $u_1 = \phi_{1x}$ satisfies the quasilinear first-order equation

$$2k\,u_{1t} + (\gamma+1)\,u_1\,u_{1x} = -f' + G_x \qquad (4.13)$$

which has characteristics $dx/dt = (\gamma+1)u_1/(2k)$. Some progress toward an analytical solution can be made in the special case $f(x) = \{(\gamma+1)\,u_{1\infty}^2/2\}\,\{1 - (x/x_1)^2\}$, $G(x,t) = \beta\,(x/x_1)\,e^{it}$. If s is measured along characteristics and r is constant along characteristics, with the choice s=t made for greatest convenience, the general solution is found to be

$$\frac{1}{x_1} x\,(r,s) = A(r)\, e^{(s-r)/\upsilon} + B(r)\, e^{-(s-r)/\upsilon} - \frac{\beta\, e^{is}}{(\gamma+1)\, u_{1\infty}^2\, (1+\upsilon^2)} \tag{4.14}$$

$$\frac{1}{|u_{1\infty}|} u(r,s) = A(r)\, e^{(s-r)/\upsilon} - B(r)\, e^{-(s-r)/\upsilon} - \frac{i\,\upsilon\,\beta\, e^{is}}{(\gamma+1)\, u_{1\infty}^2\, (1+\upsilon^2)} \tag{4.15}$$

Downstream of the shock wave the functions A(r) and B(r) can be determined if u is specified at the exit $x = x_1$, where one can define r by setting $r = s$ at $x = x_1$. If $u = O(x - x_*)$ as the sonic line $x = x_*$ is approached, then $x \to -\infty$ as $x \to x_*$ and so it is required that $B(r) = 0$; $A(r)$ can be determined by defining r to be continuous across the shock wave. The shock-wave position $r = R(s)$ is then found from the Prandtl relation, which leads to

$$u_{1u} - u_{1d} = \frac{4k}{\gamma+1} \left.\frac{\partial x}{\partial r}\right|_{r=R} \frac{dR}{ds} \tag{4.16}$$

A rather messy first-order equation is thereby obtained for R(s). In principle the behavior of the integral curves could be studied and numerical solutions obtained. For this particular limiting case, however, the value of an analytical formulation seems diminished when even an elementary example becomes so complicated.

The advantage of analytical solutions of course is the explicit representation of physical effects and their dependence on parameters for test cases having rather simple geometry. But the asymptotic solutions have to be compared with numerical solutions obtained from a set of equations which are in some sense more complete, and such numerical solutions are needed for parameter ranges which lie beyond the reach of the asymptotic solutions. Unsteady transonic cascade flows have been studied numerically using the linearized unsteady potential equation, the full unsteady potential equation, and the unsteady Euler equations (e.g., refs. 20 - 23, respectively).

The Euler solutions of references 22 and 23 were obtained for an unstaggered cascade, for parameter ranges such that a shock wave is present between successive blades, so that comparisons with the asymptotic solutions are possible. To carry out these calculations a finite-volume scheme was developed utilizing Van Leer's flux-vector splitting (ref. 24) for a moving H-mesh, with a smooth limiter to provide the desired monotonicity property. A periodicity condition was imposed ahead of and behind the cascade; an absorbing boundary condition (ref. 25) was used at the downstream computational boundary. The initial flow is described by a steady-state numerical solution, and periodic wall oscillations are introduced starting at time zero.

A comparison of numerical and analytical predictions of shock-wave motion is shown in figure 6 for parabolic blades having 2% thickness ratio, each oscillating 180° out of phase with the adjacent blades, at a reduced frequency $\tau^{-1} = 0.1$ and with small amplitude 0.1°. It is reasonable to regard this frequency as $O(\varepsilon)$, and so the comparison is made with the integral of equation (4.12). The predicted amplitudes of the shock-wave motion are about $0.05\, x_1$ and agree very closely, but there is a small discrepancy in phase. The ripples evident in the numerical solution appear to have been caused by the interpolation of the cell-averaged Mach number. Following a transient of the type discussed following equation (4.8), which in this case lasts for about one period, the mean shock-wave position becomes nearly the same as the initial steady-flow position. The agreement deteriorates with increasing amplitude, and is also found to be poor (ref. 22) for a 5% blade with 0.25° amplitude, which corresponds to a smaller (numerical) shock-wave amplitude of about $0.03\, x_1$. A partial

analytical solution for higher-order terms shows clearly that this loss of accuracy with increasing thickness should be expected. Euler solutions for a nozzle with fluctuating back pressure were also obtained in reference 26. In one comparison the calculated shock-wave position agreed closely with that predicted for the same case using the asymptotic formulation of reference 16.

For a higher frequency $\tau^{-1} = 0.5$, numerical solutions for the centerline pressure and velocity are plotted against x in figures 7 and 8, for 5% blades with oscillation amplitude 2.5°. Since the wavelength of disturbances carried downstream is no longer large, and since the pressure perturbations obviously are not of the same order as the velocity perturbations, this frequency must be regarded as O(1). The pressure distribution near $x = x_1$ calls into question the assumption that the channel solution for the pressure should approach a constant value at $x = x_1$. It may be that the inner solution (as yet unknown) for $x - x_1 = O(\varepsilon^{1/2})$ allows adjustment of the pressure to its constant value further downstream. The importance of using an absorbing condition at the downstream boundary of a relatively small computational domain is shown for the same case in figure 9. As would be expected, the effect of the downstream boundary condition on the shock-wave motion is seen to become important at the time when a reflected disturbance first reaches the shock wave. A transient again is evident, here lasting for about five periods. Analytical considerations show that a first approximation for the duration of this transient does not depend on frequency; for increased frequency, however, a constant time interval of course corresponds to a larger number of periods.

Supersonic Flow

Solutions for supersonic flow are included here because when applied to flows with Mach numbers in the transonic range, they provide a comparison which allows evaluation of the assumptions typically made in deriving solutions for transonic flow problems. Thus, whereas in transonic channel flow only one family of characteristics may be used because $u + a >> u - a$, in supersonic flow both families are employed. In addition, the jump in velocity across the wave is O(1) rather than being $O(\varepsilon)$ as in transonic channel flow. Finally, the jump in entropy Δs across a shock wave is not negligible even at lowest order when the flow is supersonic.

The unsteady flow field in a two-dimensional supercritical supersonic diffuser has been studied recently (refs. 27, 28). The formulation of the problem is similar to those channel-flow problems already discussed, but differs in some important respects. For example, if the ratio of the half height of the inlet lip to the length of the diffuser is defined as $\varepsilon^{1/2}$, then expansions of u and the thermodynamic variables proceed in integer powers of ε. The expansion for v is in odd powers of $\varepsilon^{1/2}$. For $\varepsilon << 1$, then, the channel is very long compared to its width. This results in a great mathematical simplification; for example, the lowest-order perturbation in u is independent of y. However, since the length-to-width ratio is $O(\varepsilon^{-1/2})$, then for $\varepsilon = 0.1$, say, this ratio is roughly 3 so that problems of technical interest can be considered in numerical examples. A similar formulation of this problem is considered in reference 29 for steady flow; the one described here appears to be more convenient for unsteady flows.

The relation which replaces equation (2.5) for the wall shape is, for symmetric walls,

$$y_w = \pm [1 + \varepsilon (f(x) + g(x,t))] \tag{4.17}$$

Thus, the change in area is $O(\varepsilon)$ rather than $O(\varepsilon^2)$ as in fully transonic flows. The corresponding expansion for the dimensionless (here with respect to the undisturbed velocity) velocity component u is

$$u = u_r + \varepsilon u_1 (x,t) + \varepsilon^2 u_2(x,y,t) + \ldots \tag{4.18}$$

with similar expansions for the pressure, density, temperature, etc. The v velocity component is written as

$$v = \varepsilon^{3/2} v_{3/2} (x,y,t) + \varepsilon^{5/2} v_{5/2} (x,y,t) + \ldots \tag{4.19}$$

Equation (4.18) illustrates one of the significant differences between the transonic and supersonic flow formulations in that u_r is a constant reference velocity with different values u_{ru} upstream and u_{rd} downstream of the shock wave. Here u_{ru} is the velocity of the undisturbed flow entering the diffuser and u_{rd} is the flow velocity immediately downstream of a shock wave into which the entering velocity is u_{ru}. Thus, in the limit $\varepsilon \rightarrow 0$ a uniform stream at u_{ru} enters a shock wave and emerges at u_{rd}, so that the jump in velocity across the wave $(u_{rd} - u_{ru}) = O(1)$. For nonzero ε, then, the flow velocity is expanded about u_{ru} upstream of the shock wave and about u_{rd} downstream of the shock wave; these relations are joined by the jump conditions which hold across the shock wave. Two different unsteady flow problems are considered in references 27 and 28, one for $\tau = O(1)$ and the other for $\tau = O(\varepsilon^{-1})$, where τ is defined as in earlier sections except that the undisturbed flow velocity is employed rather than a^*. Solutions are found for unsteady flow resulting from impressed oscillations in the back pressure and from oscillations in the wall shape downstream of the shock wave. The latter case allows consideration of separated flows downstream of the shock wave if the distribution of displacement thickness associated with the separated flow, represented by g(x,t) in equation (4.17), can be obtained. Asymptotic methods do not suffice for such a computation, but numerical solutions of the Navier-Stokes equations for flows with forced back-pressure oscillations are available (ref. 30), from which distributions of displacement thickness over x can be found as a function of the relative Mach number of the flow entering the wave; these are used in references 27 and 28.

The expansion for the shock-wave position x_s is

$$x = x_{so}(t) + \varepsilon x_{s1}(t) + \varepsilon^2 x_{s2}(y,t) + \ldots \tag{4.20}$$

For $\tau = O(1)$, the flow is truly unsteady and x_{so} = constant so the first time-dependent term is x_{s1}; the term truly unsteady is used to indicate the fact that the lag times associated with the propagation of signals from the walls or exit plane are very important. From equation (4.20), it is seen that for x_{so} = constant, small oscillations in shock-wave position occur for oscillations in back pressure or wall shape (eq. (4.17)) of order ε. For the case $\tau = O(\varepsilon^{-1})$, the flow is quasi-steady; that is, signals from the exit plane or the walls propagate infinitely fast compared to the period of oscillations of the back pressure or wall; the flow is composed of a series of steady-state flows, each with different boundary conditions. For this case it is found that $x_{so} = x_{so}(t)$ so that shock-wave motion with amplitude O(1) takes place for oscillations with amplitude $O(\varepsilon)$ in back pressure and wall shapes.

The equations found for the instantaneous position of the shock wave are, for each case,

$$\frac{dx_{s1}}{dt} = \tau [1 + u_{rd} - 2(\gamma-1)/(\gamma+1)]^{-1} \tilde{u}_1 (x^s_{so}, t) \qquad \tau = O(1) \tag{4.21a}$$

$$\frac{dx_{so}}{dt} = -\varepsilon\tau\frac{\gamma+1}{4}\left\{\left[\frac{u_{rd}}{M_{rd}^2 - 1} + \frac{1 - M_\infty^2(1 - u_{rd})}{M_\infty^2 - 1}\right][f(x_{so}) - f(x_{so}^s)\right.$$

$$\left. + g(x_{so},0) - g(x_{so}^s, 0)] + \frac{a_{rd}^2}{\gamma u_{rd}}\frac{\tilde{p}_{lb}(t)}{p_{rd}} + \frac{u_{rd}}{(1 - M_{rd}^2)}\tilde{g}(1,t)\right\} \qquad \tau = O(\varepsilon^{-1}) \qquad (4.21b)$$

where x_{so}^s represents the steady-state value of x_{so}; i.e., it is assumed that unsteady oscillations are imposed upon a flow initially at steady-state conditions. Also, $\tilde{u}_1$, $\tilde{g}$, and $\tilde{P}_1$ represent the differences between the quantity and its steady-state value at the same location. The subscript b on P_1 indicates that this is the exit or back pressure imposed upon the flow. It may be noted that equation (4.21a)), for the case $\tau = O(1)$, is linear, as expected for the case where oscillations are small. For this same reason, u_1 is evaluated at the lowest-order shock-wave position, x_{so}. Because the flow is truly unsteady, the equation for u_1 is complicated by the inclusion of several lag times and is not repeated here; details are given in references 27 and 28.

Equation (4.21b), which holds for $\tau = O(\varepsilon^{-1})$, is a nonlinear equation, reflecting the large-amplitude shock-wave displacement associated with $\tau >> 1$. Since the flow is quasi-steady, there are no time lags in the equation; e.g., a disturbance in back pressure at time t_o is felt by the shock wave at t_o, indicating an infinite propagation speed of disturbances based on a time scaled by the period of the impressed back pressure or wall oscillations. Another difference, not apparent in equation (4.21a) and (4.21b) because a detailed expression for u_1 in equation (4.21a) is not provided, is that in equation (4.21b) the shock location depends only upon the local cross-sectional areas at the shock wave and at the exit, whereas in u_1, and thus for x_{s1} in equation (4.21a), the detailed distribution of area is important. Finally, the nonlinear terms in equation (4.21b) provide a restoring condition such that shock-wave motion continues after all imposed oscillations are removed, until equilibrium is reached. This means that another lag time is introduced into the problem.

Although it is easy to differentiate asymptotically between solutions for $\tau = O(1)$ and those for $\tau = O(\varepsilon^{-1})$, it is not at all a simple matter to decide which should be used for a given set of physical parameters. Hence, a unified equation for shock-wave position is presented in references 27 and 28; it reproduces either equation (4.21a) or (4.21b) in the proper limit process and allows a relatively large range of physically interesting problems to be considered. Comparisons of results with completely numerical solutions (ref. 28) show that integrals of the unified differential equation reproduce numerical solutions with good accuracy.

Typical results for stationary walls but impressed oscillations in back pressure are shown in figure 10. It is seen that for the conditions chosen, the average position of the shock wave moves upstream until the shock wave is actually moving upstream of the throat of the diffuser. Finally, the decrease of the back pressure is no longer strong enough to pull the shock wave back and it is disgorged from the diffuser; i.e., an engine "unstart" occurs. For a given initial position and stable oscillation of the shock wave, it is found that such unstarts can arise if the amplitude of the impressed pressure oscillations is increased or the frequency is decreased.

Finally, using the aforementioned distributions of displacement thickness, it is possible to show self-sustained oscillations using the unified soution. That is, a quarter-cycle of oscillations of the back pressure is used to start the shock wave in motion, after which the back pressure is held constant. Under some conditions, continuing self-sustained oscillations occur. This phenomenon has

been found experimentally (e.g., ref. 31) in flows in which separation occurs downstream of the shock wave. In references 27 and 28, a model is proposed which relates the motion of the shock wave to the change in core-flow area (external to the displacement thickness) as the shock motion causes the size of the separation bubble and thus the displacement thickness to vary in magnitude. Briefly, if the core-flow area at the diffuser exit increases or decreases, with back pressure held constant, the shock wave must move downstream or upstream, respectively. Thus, as found experimentally, flow separation is a necessary prerequisite to self-sustained oscillations. Since a certain minimum shock Mach number ($M_s \approx 1.3$) must occur before the flow is separated by the shock wave, two modes are considered: mode one, in which the shock Mach number exceeds this limiting value at all times, and mode two, in which the limiting value is exceeded during only part of the cycle. In mode two, as soon as the shock Mach number decreases below the limiting value for separation, the separated-flow region is convected downstream and is rejoined with a post-shock separated region only after the shock Mach number again exceeds the minimum value for separation.

A typical result is shown in figure 11. Here, conditions are such that self-sustained oscillations do occur in mode two; both the instantaneous shock position and position of the leading edge of the separated region are shown. It is shown that the self-sustained oscillations choose their own period, independent of the period of the initiating oscillations in back pressure. An obvious conclusion from the studies is that such oscillations can be decreased or removed by removing the boundary layer downstream of the shock wave.

Shock-Wave Structure

Although the solutions discussed here are for inviscid flow in the main, it is instructive to consider flows at Reynolds numbers such that the longitudinal viscosity is important in some regions of the flow where shock waves form. This occurs at moderate Reynolds numbers such that to the desired order of approximation, the boundary layer is negligibly thin, but the Mach number is close enough to unity that the shock-wave thickness is not. A similar flow picture is seen in numerical simulations of transonic flow fields involving shock-capturing techniques when truncation errors and artificial viscosity cause a smearing of the waves; the structure of the shock-wave closely parallels that found in flows at moderate Reynolds numbers.

When the shock wave is outside the throat region, the formulation of the problem is similar to that employed for inviscid flow, but an extra shock-wave structure region must be considered (ref. 32). Thus, there is an inner shock-adjustment region in which the correction (3.7) is again found. Solutions for v are the same as those found for inviscid flow, to the desired order as is the first-order solution for u. It is only in higher-order terms in u, of order ε^2 and ε^3, that viscous corrections arise. A composite solution including equation (3.7) and the viscous-flow corrections may then be constructed, to be used as the outer solution to which solutions in the thin ($O(\varepsilon)$) inner shock-structure regions must match. As expected, the lowest-order solution in the shock-structure region is Taylor's solution for the structure of a weak shock wave. Relations for the velocity components, consisting of this and higher-order terms, are matched with the outer composite solutions to provide the terms in the equation for the location of the sonic line within the shock wave to first-order accuracy. When this equation is compared with the corresponding equation for the location of an infinitesimally thin shock wave in an inviscid flow under the same conditions, it is found that they are the same. Thus, as the longitudinal Reynolds number becomes very large, the shock wave becomes very thin until it becomes a discontinuity at the sonic line, which has not moved as the Reynolds number is changed; that is, the terms in the equation for its location are independent of Reynolds number. Moreover, as shown in reference 32, the velocity distribution within a shock wave at moderate Reynolds number is very close to that found in numerical computations when artificial viscosity and/or truncation errors cause a thickening or smearing of the wave. Hence, the practice of locating the shock wave at the sonic surface in numerical computations appears to be well justified.

In those cases where a shock wave forms in the thin regions enclosing a sonic throat, the methods employed in reference 32 cannot be used; indeed the nonlinear viscous-transonic equation for unsteady flow holds in this region (ref. 4). Since the flow is irrotational to the order considered, the first-order governing equation for unsteady flow can be written in terms of the velocity perturbation in the flow direction u_1 as follows:

$$k_s\, u_{1\bar{x}\bar{x}\bar{x}} - (u_{1\bar{x}})^2 - u_1 u_{1\bar{x}\bar{x}} + u_{1yy} - 2k u_{1\bar{x}t} = 0 \tag{4.22a}$$

$$k_s = \frac{1}{\mathrm{Re}(\varepsilon(\gamma+1))^{3/2}}\left[1 + \frac{\gamma - 1}{\mathrm{Pr}}\right] \tag{4.22b}$$

$$u = 1 + \varepsilon u_1 + \ldots \tag{4.22c}$$

where the Reynolds number Re is based upon the longitudinal viscosity (as is the Prandtl number Pr), the critical sonic speed, and the channel half-width at the throat. Equation (4.22a) is written for quasi-steady flow in the thin inner throat region with τ and the stretched independent variable $\bar{x}$ defined as

$$\tau = k^{-1}\{(\gamma+1)\,\varepsilon\}^{-1/2} \tag{4.23a}$$

$$x = ((\gamma+1)\varepsilon)^{1/2}\,\bar{x} \tag{4.23b}$$

A similarity transformation in terms of an arbitrary function of time

$$s = \bar{x} + by^2 + \beta(t) \tag{4.24a}$$

$$u_1 = z(s) + 4b^2y^2 - 2k\beta' \tag{4.24b}$$

allows equation (4.22a) to be written as a second-order differential equation in z

$$k_s z'' - z z' + 2b z + 8b^2 s = 0 \tag{4.25}$$

Equations (4.24) and (4.25) comprise the aforementioned extension (ref. 5) of the Tomotika and Tamada (ref. 1) transformation for steady flow, and in this case applied to unsteady viscous transonic flows. When $k_s \equiv 0$, the flow is inviscid up to and downstream of a shock wave in the flow; solutions to equation (4.25) include the jump conditions across the wave. For $k_s = O(1)$, thick shock waves occur and solutions to equation (4.25) must be found numerically. For $k_s << 1$, the problem is a classical singular-perturbation problem and an inner region enclosing the shock wave is required; again the lowest-order solution is the Taylor weak-shock solution. An example solution is shown in figure 12 for an unsteady decelerating flow for $\varepsilon = 0.1$, $\beta = e^{-2t}/4$ and $k_s = 0.01$ at $t = 0.35$ (steady flow at $t \to \infty$). The isotachs clearly show the location and structure of the shock wave. Details of the calculation and example flow pictures for $k_s = O(1)$ and $k_s \equiv 0$ are given in reference 4; the results are also applicable to steady flow, of course.

CONCLUDING REMARKS

The number of examples considered supports the assertion in the introduction that internal transonic flows are most amenable to solution by means of systematic asymptotic tchniques. Both steady and unsteady two-dimensional flows are included and even some three-dimensional flows,

although in one case numerical computations are required for inner regions. The flows considered have been inviscid, in the main. However, as indicated in the one example of supersonic diffuser flow, and as shown in reference 33 in the calculation for a transonic channel flow, the inclusion of a boundary layer is relatively simple, since solutions are written in terms of arbitrary wall shapes. Although the range of parameters is limited to the transonic or near-transonic regime, it is worth noting that it is quite difficult to locate shock waves for Mach numbers near one, using numerical techniques. In this regard, some of the results presented here have proven quite useful as baseline solutions for transonic flow codes. It appears that they would be useful also in formulating numerical codes for internal flows, because the various (inner) regions where important physical effects interact are located and their length scales are given.

REFERENCES

1. Tomotika, A., and Tamada, K.: Studies on two-dimensional transonic flows of compressible fluid, Part 1. Quarterly of Applied Mathematics, vol. 7, 1950, pp. 381-397.

2. Sichel, M.: The effect of longitudinal viscosity on the flow at a nozzle throat. Journal of Fluid Mechanics, vol. 25, 1966, pp. 769-786.

3. Ryzhov, O.S.: Zh. Vychisl. Mat. Mat. Fiz., vol. 8, 1968, pp. 472-479. English translation: Some properties of transonic flows of a real gas. Journal of Computational Mathematics and Mathematical Physics, vol. 8, 1968, pp. 330-342.

4. Adamson, T. C., Jr., and Richey, G. K.: Unsteady transonic flows with shock waves in two-dimensional channels. Journal of Fluid Mechanics, vol. 60, 1973, pp. 363-382.

5. Adamson, T. C., Jr.: Unsteady transonic flows in two-dimensional channels. Journal of Fluid Mechanics, vol. 52, 1972, pp. 437-449.

6. Szaniawski. A.: Transonic approximations to the flow through a nozzle. Archiwum Mechaniki Stosowanej, vol. 17 , 1965, pp. 79-85.

7. Kopystynski, J., and Szaniawski, A.: Structure of flow in a nozzle throat. Archiwum Mechaniki Stosowanej, vol. 17, 1965, pp. 453-466.

8. Adamson, T. C., Jr., Messiter, A. F., and Richey, G. K.: On the matching of solutions for unsteady transonic nozzle flows. Archiwum Mechaniki Stosowanej, vol. 26, 1974, pp. 617-628.

9. Messiter, A. F., and Adamson, T. C., Jr.: On the flow near a weak shock wave downstream of a nozzle throat. Journal of Fluid Mechanics, vol. 69, 1975, pp. 97-108.

10. Messiter, A. F., and Adamson, T. C., Jr.: Asymptotic solutions for nonsteady transonic channel flows. Symposium Transsonicum II, K. Oswatitsch & D. Rues, eds., Springer, 1976, pp. 41-48.

11. Messiter, A.F., and Adamson, T.C., Jr.: Transonic small-disturbance theory for lightly loaded cascades. AIAA Journal, vol. 19, 1981, pp. 1047-1054.

12. Kamath, H.: An analysis of the transonic flow through a lightly loaded compressor rotor. Ph.D. Thesis, The University of Michigan , 1988.

13. Kamath, H., and Adamson, T.C., Jr.: Transonic flow through a lightly loaded compressor rotor. To be submitted, 1988.

14. Adamson, T. C., Jr.: Three-dimensonal transonic shear flow in a channel. Transonic Flow Problems in Turbomachinery, T. C. Adamson, Jr. and M. F. Platzer, eds., Hemisphere, 1978, pp. 70-78.

15. Adamson, T. C., Jr., and Sichel, M.: Transonic shear flow in a three-dimensional channel. Journal of Fluid Mechanics, vol. 123 , 1982, pp. 443-457.

16. Adamson, T. C., Jr., Messiter, A. F., and Liou, M.-S.: Large-amplitude shock-wave motion in two-dimensional transonic channel flows. AIAA Journal, vol. 16, 1978, pp. 1240-1247.

17. Messiter, A. F., and Adamson, T. C., Jr.: Forced oscillations of transonic channel and inlet flows with shock waves. AIAA Journal, Vol. 22, 1984, pp. 1590-1599.

18. Chan, J. S.-K., and Adamson, T. C., Jr.: Unsteady transonic flows with shock waves in an asymmetric channel. AIAA Journal, Vol. 16, 1978, pp. 377-384.

19. Richey, G. K., and Adamson, T. C., Jr.: Analysis of unsteady transonic flow with shock waves. AIAA Journal, Vol. 14, 1976, pp. 1054-1061.

20. Verdon, J. M., and Caspar, J. R.: A linearized unsteady aerodynamic analysis for transonic cascades. Journal of Fluid Mechanics, vol. 149, 1984, pp. 403-429.

21. Shankar, V., Ide, H., and Goebel, T.: Unsteady full potential computations for complex configurations. AIAA Paper 87-0110, 1987.

22. Li, C.-C.: Unsteady transonic cascade flows. Ph.D. Thesis, The University of Michigan, 1988.

23. Li, C.-C., Messiter, A. F., and Van Leer, B.: Unsteady transonic cascade flow with in-passage shock wave. Note submitted to AIAA Journal, 1988.

24. Van Leer, B.: Flux-vector splitting for the Euler equations. Lecture Notes in Physics, vol. 170, 1982, pp. 507-512.

25. Hedstrom, G. W.: Nonreflecting boundary conditions for nonlinear hyperbolic systems, Journal of Computational Physics. vol. 30, 1979, pp. 222-237.

26. Bolcs, A., Fransson, T.H., and Platzer, M.F.: Numerical simulation of inviscid transonic flow through nozzles with fluctuating back pressure. American Society of Mechanical Engineers GT Paper, 1988.

27. Biedron, R.T.: Unsteady flow in a supercritical supersonic inlet. Ph.D. Thesis, The University of Michigan, 1988.

28. Biedron, R. T., and Adamson, T. C., Jr.: Unsteady flow in a supercritical supersonic diffuser. AIAA Paper 87-0162, 1987, to appear in AIAA Journal.

29. Lin, C. Q., and Shen, S. F.: Inviscid compressible flow with shock in two-dimensional slender nozzles. Journal of Fluid Mechanics, vol. 157, 1985, pp. 265-287.

30. Liou, M.-S.: Private communication, 1987.

31. Sajben, M., Bogar, T.J., and Kroutil, J.C.: Forced Oscillation experiments in supercritical diffuser flows. AIAA Journal, vol. 22, 1984, pp. 465-470.

32. Mace, J., and Adamson, T. C., Jr.: Shock waves in transonic channel flows at moderate Reynolds numbers. AIAA Journal, vol. 24, 1986, pp. 591-598.

33. Liou, M.-S., and Sajben, M.: Analysis of unsteady viscous transonic flow with a shock wave in a two-dimensional channel. AIAA Paper 80-1095, 1980.

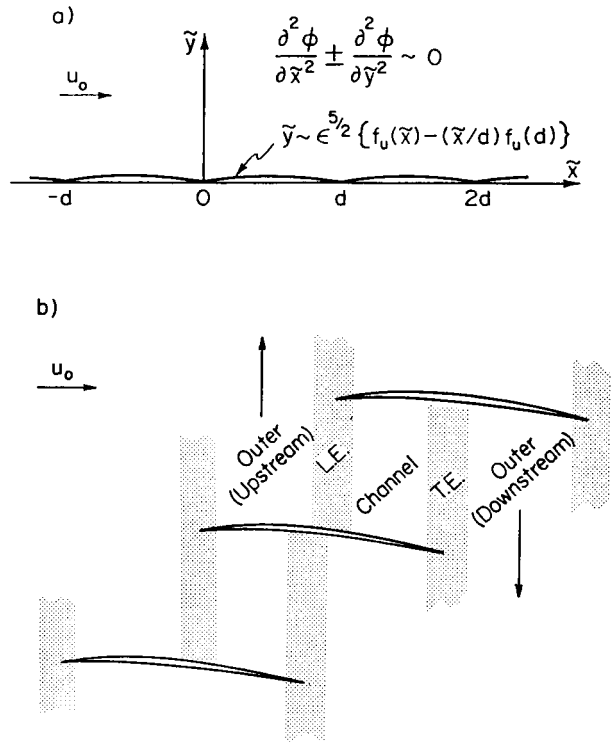

Figure 1. Asymptotic description of cascade flow. a) Approximate flow problem at large distances. b) Outer, edge, and channel flow regions.

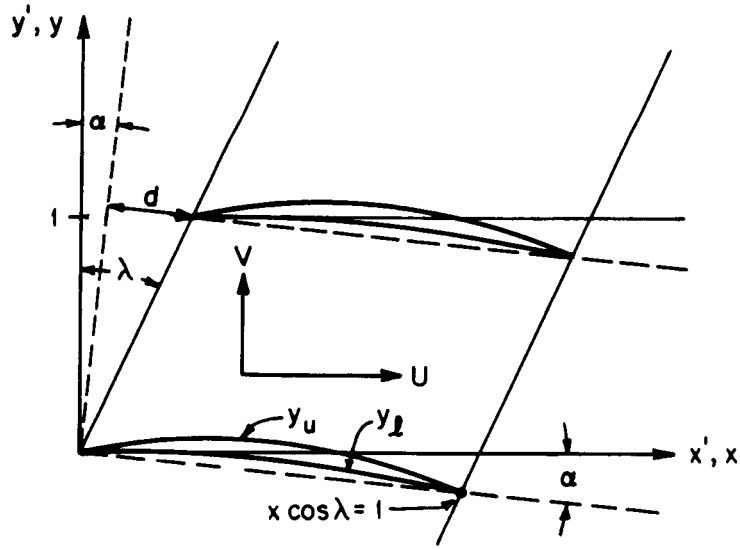

Figure 2. Sketch of two adjoining airfoils at an arbitrary radius, showing the stagger angle λ, the angle of attack α, and the notation used.

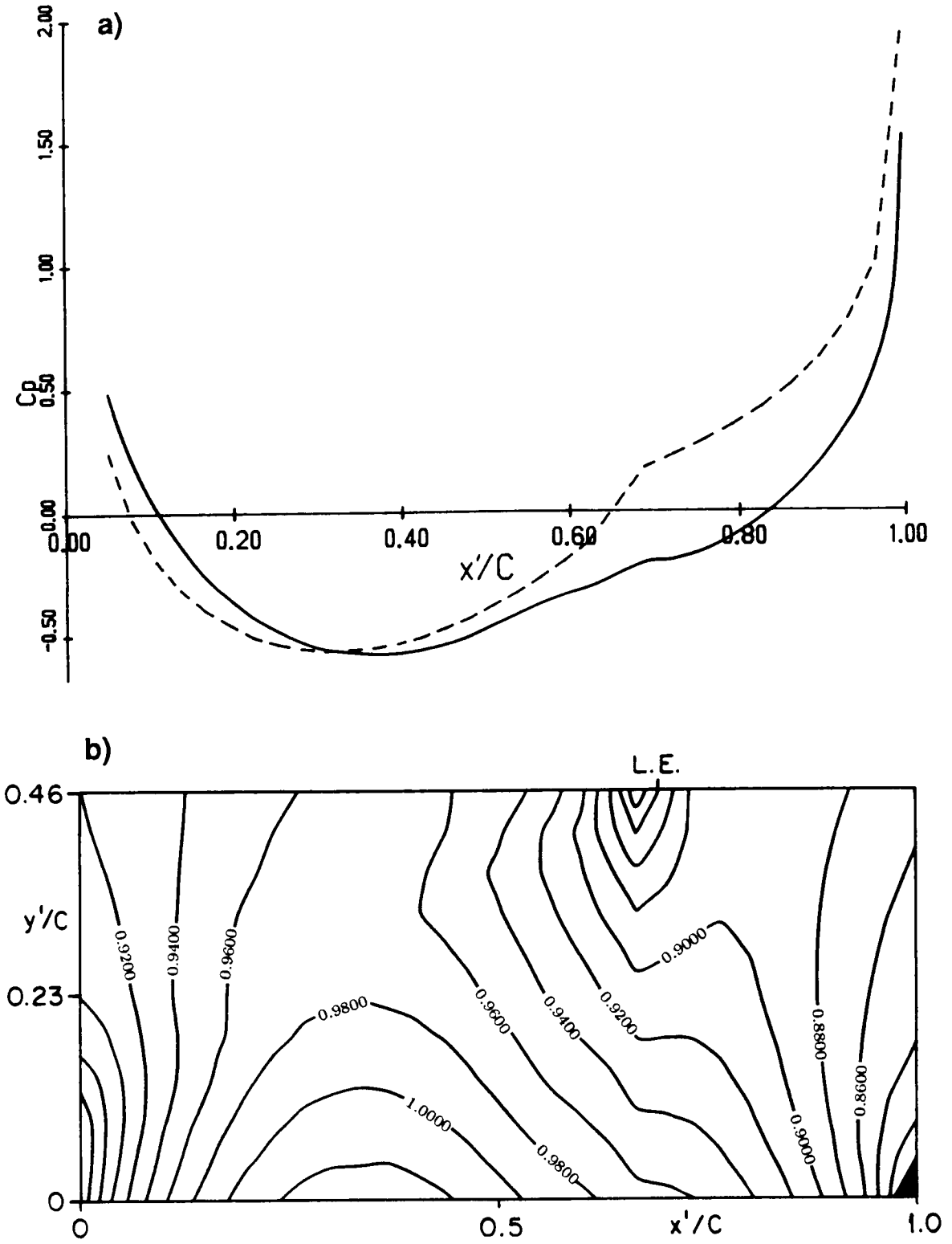

Figure 3. Calculated a) pressure distribution on the suction surface and b) lines of constant Mach number at a radial position near the tip for a compressor rotor with cambered circular-arc airfoils; t/c = 0.035, max. camber = 1/4 (t/c), axial Mach no. = 0.52, relative tip Mach no. = 0.95; 31 blades; $c_a = \delta = 0.105$, s = 1.527, $\alpha = 1.13°$, $\lambda_{tip} = 56.68°$. Dashed lines in (a) show first-order solutions only.

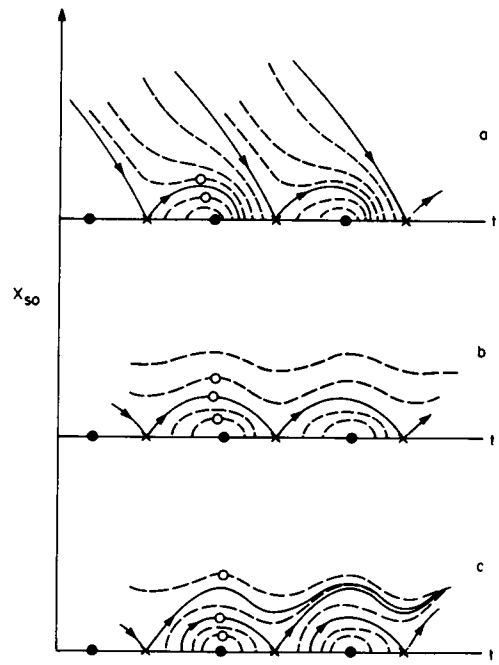

Figure 4. Sketch of possible configurations for integral curves through saddle points (——); other integral curves (----); • center; x saddle point. a) Integral curves leaving x reach time axis before next x; b) Integral curves leaving x reach time axis at next x; c) Integral curves leaving x never return to time axis. Details in reference 17.

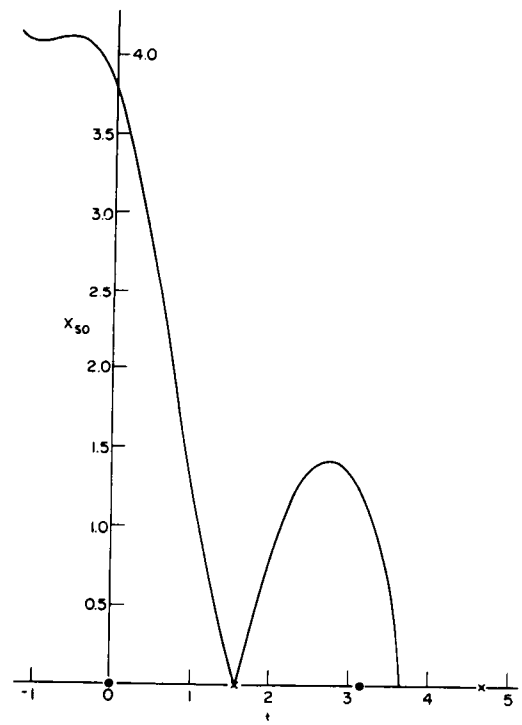

Figure 5. Calculated curve through the saddle point illustrating the case sketched in figure 4a, for $c_{2d} = 0$, $G = 4 \sin 2t$, $\gamma = 1.4$, $\tau = 100$, $\varepsilon = 0.10$. Solution found by numerical integration of equation for x_{so}. Details in reference 17.

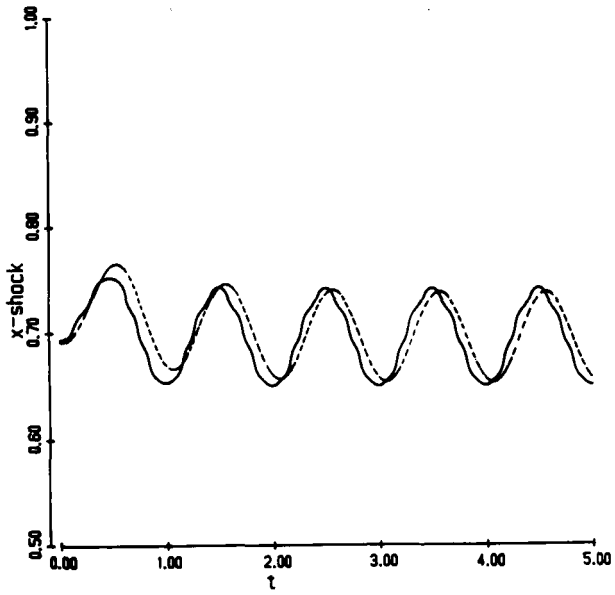

Figure 6. Numerical (——) and asymptotic (----) shock-wave displacement for unstaggered cascade with blade thickness ratio 2%, reduced frequency 0.1, and oscillation amplitude 0.1°.

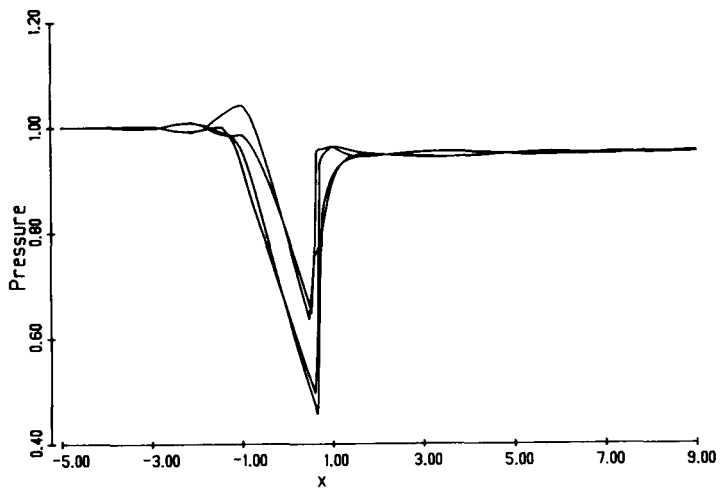

Figure 7. Calculated centerline pressure at times one-quarter period apart, for unstaggered cascade with blade thickness ratio 5%, reduced frequency 0.5, and oscillation amplitude 0.25°.

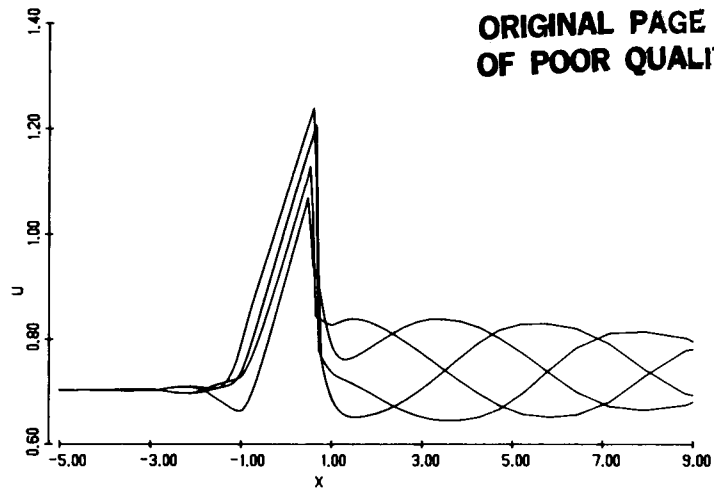

Figure 8. Calculated centerline velocity at times one-quarter period apart, for unstaggered cascade with blade thickness ratio 5%, reduced frequency 0.5, and oscillation amplitude 0.25°.

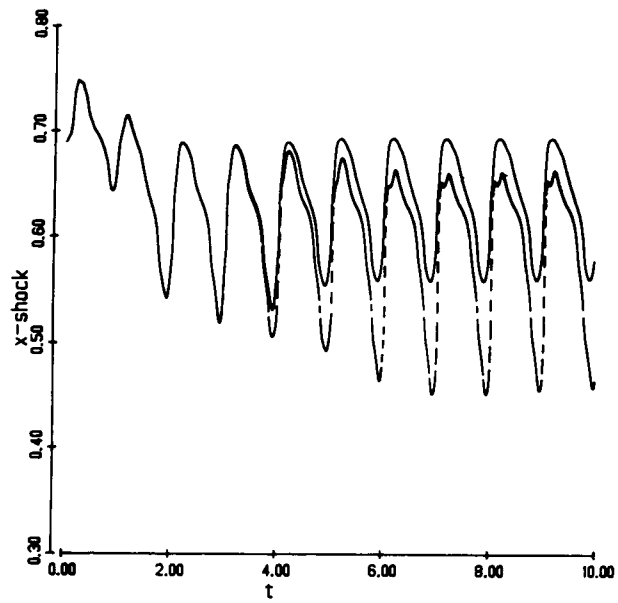

Figure 9. Effect of absorbing (——) and reflecting (----) downstream boundary conditions on shock-wave motion for unstaggered cascade with blade thickness ratio 5%, reduced frequency 0.5, and oscillation amplitude 0.25°.

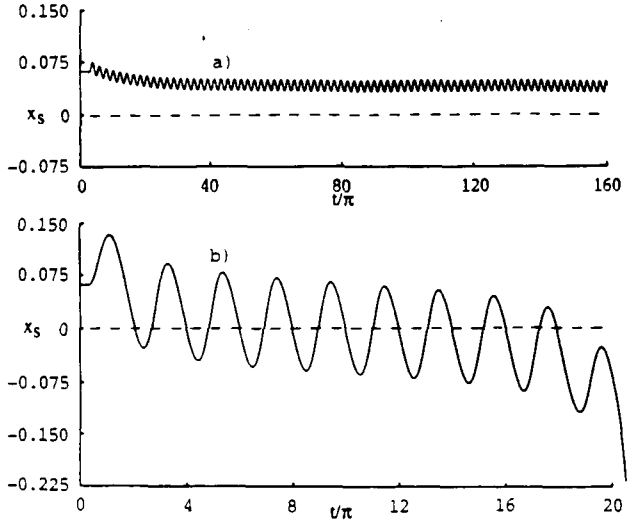

Figure 10. Effect of frequency of back-pressure oscillations on shock-wave response. Dashed line denotes diffuser throat; h = 1 ft., L = 12.65 ft., $x_s^s = 0.062$, $u_\infty = 1400$ ft./sec., $M_\infty = 1.50$, $\varepsilon = 0.00625$, $\Delta p_b/p_o = -0.03 \sin 2\pi f_r t$; a) $f_r = 80$ Hz, $\tau = 0.22$; b) $f_r = 10$ Hz, $\tau = 1.76$. Details in reference 29.

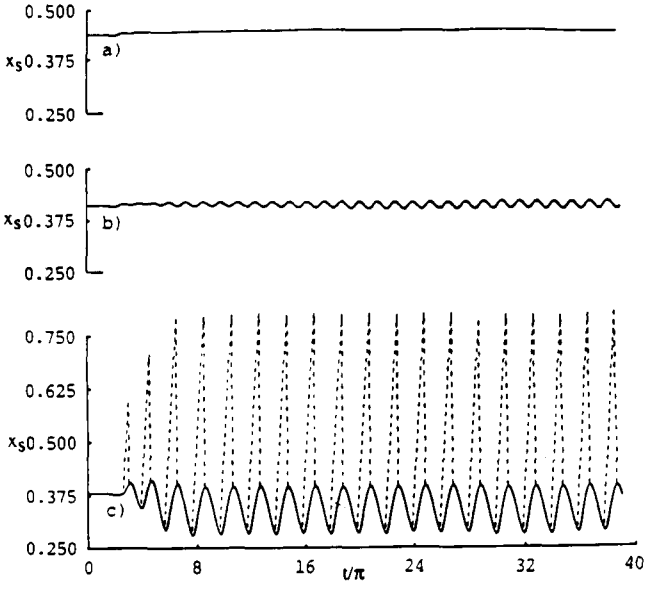

Figure 11. Effect of initial shock-wave position on self-sustained oscillations. a) $x_s^s = 0.442$; b) $x_s^s = 0.415$; c) $x_s^s = 0.379$. In curve c) dashed line indicates location of separation point (Mode 2). Throat is at 0.30. Details in reference 29.

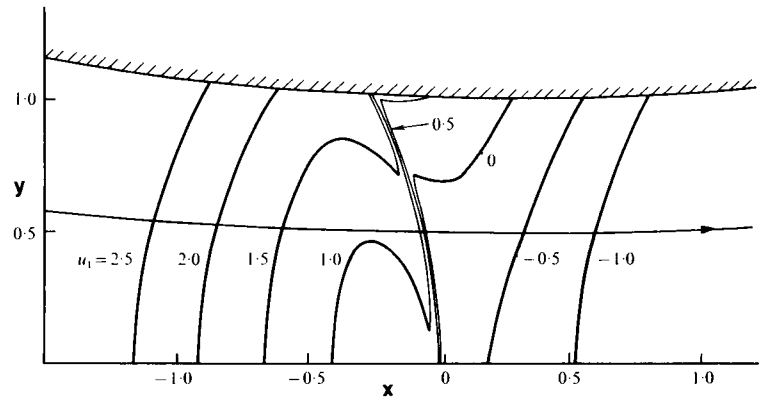

Figure 12. Flow picture for thin shock in unsteady decelerating flow showing isotachs and a streamline at t = 0.35; $k_s = 0.01$, $\beta = (1/4)\, e^{-2t}$, $\varepsilon = 0.1$, $\gamma = 1.4$. Details in reference 4.